

K^* Mesons and Nucleon Strangeness

L.L. Barz^{1,2}, H. Forkel^{3,4}, H.-W. Hammer^{5,6}, F.S. Navarra¹, M. Nielsen¹, and M.J. Ramsey-Musolf^{6,7*}

¹*Instituto de Física, Universidade de São Paulo
C.P. 66318, 05315-970 São Paulo, SP, Brazil*

²*Faculdade de Engenharia de Joinville, Universidade Estadual de Santa Catarina
82223-100 Joinville, SC, Brazil*

³*European Centre for Theoretical Studies in Nuclear Physics and Related Areas,
Villa Tambosi, Strada delle Tabarelle 286, I-38050 Villazzano, Italy*

⁴*Institut für Theoretische Physik, Universität Heidelberg,
Philosophenweg 19, D-69120 Heidelberg, Germany*

⁵ *TRIUMF, 4004 Wesbrook Mall, Vancouver, B.C., Canada V6T 2A3*

⁶ *Institute for Nuclear Theory, University of Washington, Seattle, WA 98195, USA*

⁷ *Department of Physics, University of Connecticut, Storrs, CT 08629 USA*

Abstract

We study contributions to the nucleon strange quark vector current form factors from intermediate states containing K^* mesons. We show how these contributions may be comparable in magnitude to those made by K mesons, using methods complementary to those employed in quark model studies. We also analyze the degree of theoretical uncertainty associated with K^* contributions.

PACS numbers: 14.20.Dh, 12.40.-y

*National Science Foundation Young Investigator

I. INTRODUCTION

The role played by virtual $q\bar{q}$ pairs in the low-energy structure of hadrons remains one of the outstanding questions for hadron structure physics. Despite the evidence for important $q\bar{q}$ sea effects obtained with deep inelastic scattering, the experimental manifestations of explicit sea-quark effects at low energies are minimal. Partial explanations for this absence have been given using a non-relativistic quark model framework by the authors of Ref. [1], who noted that in the adiabatic approximation, virtual $q\bar{q}$ pairs renormalize the string tension and, therefore, do not have any discernable impact on the low-lying spectrum of hadronic states. Similarly, virtual $q\bar{q}$ effects – in the guise of virtual mesonic loops – which could conceivably lead to large $\rho - \omega$ and $\phi - \omega$ mixing were shown to cancel at second order in strong couplings when a sum is performed over a tower of virtual hadronic states [2]. The latter result provides insight into the applicability of the OZI Rule to V - V' mixing despite the naïve scale of $q\bar{q}$ effects expected at one-loop order.

Nevertheless, several mysteries involving $q\bar{q}$ pairs remain to be solved. Of particular interest are those involving nucleon matrix elements of strange quark operators, $\langle N | \bar{s} \Gamma s | N \rangle$. The latter explicitly probe properties of the $q\bar{q}$ sea at low energies, since the nucleon contains no valence strange quarks. Moreover, the mass scale associated with $s\bar{s}$ pairs – $m_s \sim \Lambda_{QCD}$ – implies that such pairs live for sufficiently long times and propagate over sufficiently large distances to produce observable effects when probed explicitly. In this respect, $s\bar{s}$ pairs stand in contrast with, *e.g.*, $c\bar{c}$ pairs, whose effects one expects to be suppressed by powers of $\Lambda_{QCD}/m_c \sim 0.1$ [3].

Some support for these simple-minded expectations is provided by determinations of $\langle N | \bar{s} s | N \rangle$ from the πN “sigma” term [4] and of $\langle N | \bar{s} \gamma_\mu \gamma_5 s | N \rangle$ from polarized deep inelastic scattering [5] and neutrino-nucleus quasi-elastic scattering [6]. The former suggests that roughly 15% of the nucleon mass is generated by $s\bar{s}$ pairs, while the latter implies that strange quarks contribute about 30% of the total quark contribution to the nucleon spin¹. Measurements of $\langle N | \bar{s} \gamma_\mu s | N \rangle$, which would provide information about the strange quark contribution to the nucleon magnetic moment and rms radius are presently underway at MIT-Bates [7], Mainz [8], and the Jefferson Laboratory [9]. The first results for the strangeness magnetic form factor have been reported in Ref. [7]. One expects this set of $\langle N | \bar{s} \Gamma s | N \rangle$ determinations to provide a clearer picture of the $q\bar{q}$ sea than obtained from existing spectroscopic data alone.

Despite over a decade of theoretical efforts to study nucleon strangeness, the theoretical understanding of s-quark matrix elements remains in its infancy. In the case of $\langle N | \bar{s} \gamma_\mu s | N \rangle$, a plethora of predictions have been reported in the literature [10–18]. While a few lattice results have been obtained by different groups [10], they are not entirely consistent with each other nor with the recent first results for the “strange magnetic moment” obtained by the SAMPLE collaboration [7]. The remaining predictions – based generally on QCD-inspired nucleon models [11,14] or low-energy truncations of QCD in a hadronic basis [12,13,15] –

¹Theoretical uncertainties associated with SU(3) breaking qualify the conclusions drawn from deep inelastic scattering experiments, however.

display a broad range in magnitude and sign. Recently, it has been shown why such truncations – either in the strong coupling constant (g) expansion (loop order) [16,17] or hadronic excitation energy (ΔE) [14] – are untrustworthy and may produce misleading results. The implication of these studies is that the intuitively appealing picture of a kaon cloud around the nucleon does not suffice to describe $s\bar{s}$ fluctuations in the nucleon. It appears that one must include both the full set of virtual hadronic intermediate states [14] as well as the full set of higher-order rescattering effects for a given state [16,17] in order to obtain a physically realistic prediction. In principle, corrections to the leading order truncations in ΔE and g could be accounted for by the appropriate low-energy constants in chiral perturbation theory (CHPT); however, chiral symmetry does not afford a determination of the low-energy constant relevant to nucleon vector current strangeness [15]. Hence, one must understand in some detail the short-distance strong interaction mechanisms responsible for the low-energy structure of the strange quark sea.

In the present study, we amplify on the themes of Refs. [14–17] by studying the K^* contribution to $\langle N|\bar{s}\gamma_\mu s|N\rangle$. Our objective is two-fold: (i) to illustrate, using an alternative framework to that of Ref. [14], how inclusion of higher-lying intermediate states may alter conclusions obtained when only the lightest “OZI-allowed” fluctuation is included, and (ii) to demonstrate the theoretical uncertainty associated with computing higher-lying contributions. For these purposes, we restrict ourselves to second order in the strong meson-baryon coupling, g , when treating hadronic amplitudes $N \rightarrow YK^*$ *etc.*, fully cognizant of the shortcomings such a truncation entails. In fact, the kind of analysis of higher-order effects reported in Ref. [17] for the $K\bar{K}$ intermediate state does not appear feasible at present for higher lying states. Consequently, some form of model-dependent truncation is necessary when treating these states, and we do not, therefore, pretend to make any reliable numerical predictions. Rather, we use the $\mathcal{O}(g^2)$ (one-loop) truncation to illustrate the two main points stated above. In this respect, our study is similar in spirit to that of Ref. [18], where a comparison at one-loop order was made to show that contributions from intermediate states containing no valence strangeness (3π) and those containing valence s-quarks ($K\bar{K}$) may be comparable in magnitude.

In order to estimate the degree of theoretical uncertainty one has in the numerical prediction for the K^* contribution, we use two approaches to carry out the calculation: (a) an explicit one-loop calculation, where form factors are included at hadronic vertices and the intermediate state $\bar{s}\gamma_\mu s$ matrix elements are taken to be point-like, and (b) a computation using dispersion relations, in which the $N\bar{N} \rightarrow KK, KK^*, K^*K^*$ amplitudes are computed in the Born approximation but form factors are included at the $\bar{s}\gamma_\mu s$ insertions. These computations are outlined, respectively, in Sections II and III. In Section IV, we discuss the results of the calculations and compare with the conclusions drawn in Ref. [14].

II. ONE-LOOP CALCULATION

The first “kaon cloud” estimates of $\langle N|\bar{s}\gamma_\mu s|N\rangle$ were obtained from the amplitudes associated with the diagrams of Fig. 1, where only the contributions for $B = B' = \Lambda, \Sigma$ and $M = M' = K$ were included [13]. Here we consider the next heaviest contributions by including the octet of spin-one mesons as well as the pseudoscalars, and compute the

following amplitudes where, in each case, $B = B' = \Lambda$ or Σ : (1a) for $M = K^*$; (1b) for $M = M' = K^*$; (1b) for $M = K$, $M' = K^*$; (1c) for $M = K^*$. As we discuss below, the diagrams (1c) are required for consistency with the Ward-Takahashi identities.

The resulting contributions to the strange-quark vector current matrix element are embodied in the Dirac and Pauli form factors defined via

$$\langle N(p') | \bar{s} \gamma_\mu s | N(p) \rangle = \bar{U}(p') \left[F_1^{(s)}(q^2) \gamma_\mu + i \frac{\sigma_{\mu\nu} q^\nu}{2m_N} F_2^{(s)}(q^2) \right] U(p) \quad , \quad (1)$$

where $U(p)$ denotes the nucleon spinor. Recall that $F_1^{(s)}(0) = 0$, due to the zero strangeness charge of the nucleon. The leading nonvanishing moments of the corresponding Sachs form factors

$$G_E^{(s)}(q^2) = F_1^{(s)}(q^2) + \frac{q^2}{4m_N^2} F_2^{(s)}(q^2), \quad (2)$$

$$G_M^{(s)}(q^2) = F_1^{(s)}(q^2) + F_2^{(s)}(q^2) \quad (3)$$

are the strangeness radius

$$\langle r_s^2 \rangle_S = 6 \frac{d}{dq^2} G_E^{(s)}(q^2) \Big|_{q^2=0} \quad , \quad (4)$$

and the strangeness magnetic moment

$$\mu_s = G_M^{(s)}(0) = F_2^{(s)}(0) \quad . \quad (5)$$

For future reference, we note that the Sachs radius $\langle r_s^2 \rangle_S$ is related to the corresponding Dirac radius as

$$\langle r_s^2 \rangle_S = \langle r_s^2 \rangle_D + \frac{3}{2m_N^2} \mu_s \quad . \quad (6)$$

In order to extend the $K - \Lambda$ loop framework to include K^* -meson contributions, we start from the meson baryon effective lagrangians

$$\mathcal{L}_{MB} = -i g_{ps} \bar{B} \gamma_5 B K \quad , \quad (7)$$

$$\mathcal{L}_{VB} = -g_v (\bar{B} \gamma_\alpha B V^\alpha + \frac{\kappa}{2m_N} \bar{B} \sigma_{\alpha\beta} B \partial^\alpha V^\beta) \quad , \quad (8)$$

where B , K , and V^α are the baryon, kaon, and K^* vector-meson fields respectively, $m_N = 939$ MeV is the nucleon mass and κ is the ratio of tensor to vector coupling, $\kappa = g_t/g_v = 3.26$, with $g_v/\sqrt{4\pi} = -1.588$ [19]. The strength of the pseudoscalar coupling is $g_{ps}/\sqrt{4\pi} = -3.944$ [19].

In order to account in some way for the finite extent of the hadrons appearing in the loops of Fig. 1, we include form factors at the hadronic vertices. For simplicity, we adopt a monopole form

$$F(k^2) = \frac{m^2 - \Lambda^2}{k^2 - \Lambda^2} \quad . \quad (9)$$

Although there is no rigorous justification for this choice, form factors of this type for the KNA and $K^*N\Lambda$ vertices are used in the Bonn potential. Their cut-off parameters are determined from hyperon-nucleon scattering data [19]: $\Lambda_{K^*} = 2.2$ (2.1), $\Lambda_K = 1.2$ (1.4) GeV with masses $m_K = 495$ MeV and $m_{K^*} = 895$ MeV [20]. The numbers in parenthesis denote values obtained in an alternate model for the baryon-baryon interaction. The momentum of the K^* is k . These form factors render all the following loop integrals finite and reproduce the on-shell values of the mesonic couplings (since $F(m^2) = 1$) .

In the presence of electroweak fields the non-local meson-baryon interaction of Eqs. (7-9) gives rise to vertex currents. In order to maintain gauge invariance we introduce the photon field by minimal substitution of the momentum variable in the form factors². This procedure generates the nonlocal seagull vertex [21,22,15]

$$i\Gamma_{\mu\alpha}^{(s)}(k, q) = ig_v Q_{K^*} (q \pm 2k)_\mu \frac{F(k^2) - F((q \pm k)^2)}{(q \pm k)^2 - k^2} \left[\pm \gamma_\alpha + \frac{i\kappa}{2m_N} \sigma_{\alpha\beta} k^\beta \right], \quad (10)$$

where the upper/lower signs correspond to an incoming/outgoing vector meson (with index α), $Q_{K^*} = -1$ is the K^* strangeness charge, and q is the photon momentum.

Due to the derivative in eq. (8), the minimal substitution also generates an additional seagull vertex (even in the absence of meson-nucleon form factors)

$$i\Gamma_{\mu\alpha}^{(v)}(k) = \pm \frac{g_v \kappa Q_{K^*}}{2m_N} F((q \pm k)^2) \sigma_{\alpha\mu}, \quad (11)$$

where the sign convention is the same as above.

The diagonal matrix elements of $\bar{s}\gamma_\mu s$ for strange mesons and baryons is straightforwardly determined by current conservation and the net strangeness charge of each hadron. The structure of the s-quark current spin-flip transition from K to K^* is

$$\langle K_a^*(k_1, \varepsilon) | \bar{s}\gamma_\mu s | K_b(k_2) \rangle = \frac{F_{KK^*}^{(s)}(q^2)}{m_{K^*}} \epsilon_{\mu\nu\alpha\beta} k_1^\nu k_2^\alpha \varepsilon^{*\beta} \delta_{ab}, \quad (12)$$

where a and b are isospin indices, ε^β is the polarization vector of the K^* , and k_1, k_2 are the meson momenta. In a loop calculation, $F_{KK^*}^{(s)}(q^2)$ is taken to be a constant equal to its value at the photon point. In order to estimate this constant, we follow Ref. [23] and assume $F_{KK^*}^{(s)}(q^2)$ to be dominated at low- q^2 by the lightest $I^G(J^{PC}) = 0^-(1^{--})$ vector mesons³:

$$\frac{F_{KK^*}^{(s)}(q^2)}{m_{K^*}} = - \sum_{V=\omega, \phi} \frac{G_{K^*VK} S_V}{q^2 - m_V^2}, \quad (13)$$

where G_{K^*VK} are the couplings of the vector meson V to K and K^* . S_V determines the strength of the strange-current conversion into V :

²As noted in [21,15] and elsewhere this procedure is not unique since the Ward-Takahashi identity does not restrict the transverse part of the vertex.

³The validity of this assumption is discussed in more detail in the following section.

$$\langle 0|\bar{s}\gamma_\mu s|V\rangle = S_V\varepsilon_\mu = \frac{m_V^2}{f_V} \frac{f_V}{f_V^{(s)}}\varepsilon_\mu. \quad (14)$$

From the known isoscalar electromagnetic couplings $f_{\omega,\phi}$ one can delineate the corresponding strange-current couplings with the help of a simple quark counting prescription based on flavor symmetry [12]:

$$\frac{f_\omega}{f_\omega^{(s)}} = -\sqrt{6}\frac{\sin \epsilon}{\sin(\theta_0 + \epsilon)}, \quad \frac{f_\phi}{f_\phi^{(s)}} = -\sqrt{6}\frac{\cos \epsilon}{\cos(\theta_0 + \epsilon)}, \quad (15)$$

Here $\epsilon = 0.053$ [24] is the mixing angle between the pure $\bar{u}u + \bar{d}d$ and $\bar{s}s$ states and the physical vector mesons ω and ϕ , and θ_0 is the “magic angle” defined by $\sin^2 \theta_0 = 1/3$. From the above we find $f_\omega/f_\omega^{(s)} = -0.21$ and $f_\phi/f_\phi^{(s)} = -3.11$. Combined with the strong couplings $G_{K^*\phi K} = -8.94 \text{ GeV}^{-1}$ and $G_{K^*\omega K} = 6.84 \text{ GeV}^{-1}$ estimated in Ref. [23] we finally obtain

$$F_{KK^*}^{(s)}(0) = 1.84. \quad (16)$$

After these preparations⁴, we can evaluate the K^* loop contributions to the nucleon’s strangeness radius and magnetic moment. Explicit expressions for the loop amplitudes are given in Appendix A. The results for the different diagrams are listed in Table I. The implications of these results are discussed in Section IV.

III. DISPERSION RELATION CALCULATION

An alternative approach to computing virtual hadronic contributions to strange quark form factors is the use of dispersion relations (DR’s). In principle, DR’s provide a method for including information beyond second order in g , both via the strong amplitudes $N \rightarrow YK^* \rightarrow N$ and through the form factors $F_n^{(s)}$ describing the intermediate state matrix elements $\langle Y|\bar{s}\gamma_\mu s|Y\rangle$, $\langle K^*|\bar{s}\gamma_\mu s|K\rangle$, \dots . The one-loop calculation of Section II is equivalent to the use of a DR in which the strong amplitudes $N \rightarrow YK^* \rightarrow N$ are computed in the Born approximation and the form factors assumed to be point-like: $F_n^{(s)}(q^2) = F_n^{(s)}(0) = \text{const}^5$.

The inclusion of rescattering and resonance effects in the $N \rightarrow YK^* \rightarrow N$ amplitude would require the existence of sufficient data for $KN \rightarrow NK\pi, \dots$ or $N\bar{N} \rightarrow KK\pi, KK\pi\pi$ *etc.* to permit analytic continuation of these amplitudes to the unphysical regime as needed for the dispersion relation. Although such a program is feasible to some degree for the $K\bar{K}$ intermediate state [17], it does not appear practical at present for the case of higher mass

⁴Note also that the small SU(3) values for the ΣKN couplings [19] lead to a strong suppression of the contributions from ΣK intermediate states [13]. This argument does not affect, however, the Σ^*K and Σ^*K^* contributions.

⁵The equivalence holds only when the hadronic form factors of Eq. (9) are set to unity.

strange mesons of interest here. Consequently, we include the amplitude for $N \rightarrow YK^* \rightarrow N$ at the level of the Born approximation. In the case of the $F_n^{(s)}(q^2)$, however, it is possible to introduce some structure beyond the point-like approximation, albeit in a model-dependent way. Our strategy for doing so is discussed below.

First, we review the formalism for treating strangeness form factors with DR's. We write an unsubtracted dispersion relation for the Pauli form factor $F_2^{(s)}$ and subtract the one for the Dirac form factor $F_1^{(s)}$ once at $t = 0$ (where $F_1^{(s)}$ vanishes, see above):

$$F_1^{(s)}(t) = \frac{t}{\pi} \int_{t_0}^{\infty} dt' \frac{\text{Im } F_1^{(s)}(t')}{t'(t' - t)}, \quad (17)$$

$$F_2^{(s)}(t) = \frac{1}{\pi} \int_{t_0}^{\infty} dt' \frac{\text{Im } F_2^{(s)}(t')}{t' - t},$$

where $t \equiv q^2$. The cut along the real t -axis starts at the threshold t_0 of a given multi-particle intermediate state, as *e.g.* $t_0 = 4m_K^2$ for the $K\bar{K}$ state. From Eqs. (17) one expects that contributions from the lightest intermediate states will mainly determine the behavior of the form factors at $t = 0$. The imaginary part of the form factors is readily obtained by means of a spectral decomposition. Since the matrix elements $\langle N(p) | \bar{s}\gamma_\mu s | N(p') \rangle$ and $\langle N(p); \bar{N}(\bar{p}) | \bar{s}\gamma_\mu s | 0 \rangle$ are simply related by crossing symmetry, we write the spectral decomposition for the latter one as [17],

$$\text{Im } \langle N(p); \bar{N}(\bar{p}) | \bar{s}\gamma_\mu s | 0 \rangle = \text{Im } \bar{U}(p) \left[F_1^{(s)}(t)\gamma_\mu + i \frac{\sigma_{\mu\nu}(p + \bar{p})^\nu}{2m_N} F_2^{(s)}(t) \right] V(\bar{p}) \quad (18)$$

$$\rightarrow \frac{\pi}{\sqrt{Z}} (2\pi)^{3/2} \mathcal{N} \sum_n \langle N(p) | \bar{J}_N(0) | n \rangle \langle n | \bar{s}\gamma_\mu s | 0 \rangle V(\bar{p}) \delta^4(p + \bar{p} - p_n),$$

where \mathcal{N} is a spinor normalization factor, Z is the nucleon's wave function renormalization constant, and $J_N(x)$ is a nucleon source. Nonzero contributions arise only from physical states $|n\rangle$ with the same quantum numbers as the current $\bar{s}\gamma_\mu s$, *i.e.* $I^G(J^{PC}) = 0^-(1^{--})$ and zero baryon number. These asymptotic states $|n\rangle$ in the above sum do not explicitly contain resonances. Resonance contributions arise via the matrix elements $\langle N(p) | \bar{J}_N(0) | n \rangle$ and $\langle n | \bar{s}\gamma_\mu s | 0 \rangle$. In the vector meson dominance approximation, one assumes the product of the two matrix elements in Eq. (18) to be strongly peaked near vector meson masses. This approximation has been used in several pole analyses of the strange vector form factors [12].

The lightest contributing intermediate states are purely mesonic: 3π , 5π , 7π , $K\bar{K}$, $K\bar{K}\pi$, 9π , $K\bar{K}\pi\pi$, \dots , in order. Intermediate baryon states $N\bar{N}$, $\Lambda\bar{\Lambda}$, \dots appear with significantly higher thresholds, t_0 . In the present study, we restrict ourselves to the strange states and consider corrections to the $K\bar{K}$ state. The first such corrections (in order of threshold) are those involving the $K\bar{K}\pi$ and $K\bar{K}\pi\pi$ intermediate states. In the previous section, these states were included using the narrow resonance approximation: $K\bar{K}\pi \rightarrow K^*\bar{K}$ and $K\bar{K}\pi\pi \rightarrow K^*\bar{K}^*$. In order to make contact with the loop results of Section II as well as with the calculation of Ref. [14] where in effect the same approximation was made, we adopt the narrow resonance approximation here. We also include the $\Lambda\bar{\Lambda}$ and $\Sigma\bar{\Sigma}$ intermediate states, even though they are not among the lightest in the series, in order to compare the DR results with those of the loop and quark model calculations, which contain these states.

As noted earlier, we also include the strong amplitudes $\langle N | \bar{J}_N(0) | n \rangle$ at the level of the Born approximation. For the matrix elements $\langle n | \bar{s} \gamma_\mu s | 0 \rangle$, parameterized by form factors $F_n^{(s)}(t)$, we go beyond the point-like approximation,

$$F_n^{(s)}(t) \equiv F_n^{(s)}(0) \equiv F_n^0, \quad (19)$$

of the one-loop and quark model calculations by allowing for some structure in the form factors. For the mesonic intermediate states, we make a simple vector meson dominance (VMD) *ansatz*. This *ansatz* is well justified for the $K\bar{K}$ state, following from $e^+e^- \rightarrow K\bar{K}$ cross section data [25] and simple flavor rotation arguments [12]. The $e^+e^- \rightarrow K\bar{K}$ data indicates a strong peak in the vicinity of the ϕ resonance, with a subsequent rapid fall-off as q^2 (time-like) increases away from m_ϕ^2 . Inclusion of a VMD-type form factor peaked near the ϕ -resonance significantly affects the $K\bar{K}$ component of the spectral functions [Eqs. (18)] and the resulting contribution to the strangeness moments as compared with the use of a point-like form factor.

In the case of the $KK\pi \sim KK^*$ and $KK\pi\pi \sim K^*K^*$ states, we take the $F_n^{(s)}(t)$ to be dominated by either the $\phi(1020)$ or the $\phi'(1680)$. Following Ref. [16] we write

$$|F_n^{(s)}(t)_{VDM}| = F_n^0 \left\{ \frac{(\xi^2)^2 + M^2\Gamma^2}{[(\xi^2 - t)^2 + M^2\Gamma^2]} \right\}^{1/2}, \quad (20)$$

where $M = m_\phi = 1020$ MeV or $m_{\phi'} = 1680 \pm 20$ MeV, $\Gamma = \Gamma_\phi = 4.43 \pm 0.05$ MeV or $\Gamma_{\phi'} = 150 \pm 50$ MeV are the total widths of the ϕ or ϕ' [20], and $\xi^2 \equiv M^2 - \Gamma^2/4$. As we note below, we need only the magnitude of the form factor in the present calculation, as the $n \rightarrow N\bar{N}$ amplitudes are real in the Born approximation. Because the states $KK\pi \sim KK^*$ and $KK\pi\pi \sim K^*K^*$ contribute to the DR of Eq. (17) for $t_0 > m_\phi$, we expect higher mass vector mesons to play a significant role in the $F_n^{(s)}(t)$ in the region of integration.

The case for ϕ' dominance is most convincing for the $K\bar{K}\pi$ intermediate state. Data for $\sigma(e^+e^- \rightarrow K_S^0 K^\pm \pi^\mp)$ in the range $1.4 \leq \sqrt{s} \leq 2.18$ GeV display a pronounced peak near $\sqrt{s} = 1.680$ GeV [26]. Furthermore, Dalitz plot analyses imply that the final state is dominated by a $K^*K \leftrightarrow KK\pi$ resonance. The OZI rule implies that the ϕ' is nearly a pure $s\bar{s}$ state, while SU(3) relations and data for $\sigma(e^+e^- \rightarrow \rho\pi; \sqrt{s} \approx 1.65)$ constrain the $\omega' - \phi'$ mixing angle to deviate by less than 10° from ideal mixing [27]. While the tails of the $\rho(770)$, $\omega(780)$, and $\phi(1020)$ affect details of the peak structure, the dominant effect is that of the ϕ' [27]. In the absence of any other structure in $\sigma(e^+e^- \rightarrow KK\pi)$ in the region $t > t_0$, we conclude that $F_{KK^*}^{(s)}(t)$ should also be dominated by the $\phi'(1680)$. Indeed, the $\omega\phi$ model of Eq. (13), which is credible for low- t , is inconsistent with annihilation data for $t > t_0$. Using it in this region would generate an artificial suppression of the $KK\pi$ spectral function.

With these considerations in mind, it is straightforward to determine the normalization $F_{KK^*}^0$ appearing in Eq. (20). Following the notation of Ref. [23], we obtain

$$F_{KK^*}^0 = G_{KK^*\phi'} m_{K^*} / f_{\phi'}^{(s)}, \quad (21)$$

where $1/f_{\phi'}^{(s)} \approx -3/f_{\phi'}$, and $G_{KK^*\phi'}$ is the strong $\phi' \rightarrow KK^*$ coupling. The latter may be obtained from $\Gamma(\phi' \rightarrow KK^*)$ which, for a single final charge state is [23]

$$\Gamma(\phi' \rightarrow KK^*) = \frac{|G_{KK^*\phi'}|^2}{12\pi} |k_F|^3 \quad , \quad (22)$$

where $k_F = 463$ MeV is the K or K^* CM momentum. Assuming $\Gamma(\phi' \rightarrow \text{all})$ is dominated by $\Gamma(\phi' \rightarrow KK^*)$ [20], we obtain $|G_{KK^*\phi'}| \approx 3.8$ GeV⁻¹.

Similarly, the ϕ' electronic width determines $f_{\phi'}$:

$$\Gamma(\phi' \rightarrow e^+e^-) = \frac{4\pi}{3} \alpha^2 \frac{M_{\phi'}^2}{f_{\phi'}^2} \quad . \quad (23)$$

Analyses of e^+e^- data yield $\Gamma(\phi' \rightarrow e^+e^-) = 0.7$ keV [27,30], from which we obtain $f_{\phi'} \approx 23$. The factor of -3 appearing in the relation between $f_{\phi'}$ and $f_{\phi'}^{(s)}$ assumes ideal mixing [see Eq. (15)]. Allowing for a small deviation $|\epsilon| < 10^\circ$ does not change our results appreciably, especially since the ω' is not observed to decay to $KK\pi$.

Substituting these results into Eq. (21) yields $F_{KK^*}^0 = F_{KK^*}^{(s)}(0) = 0.43$, to be compared with the value $F_{KK^*}^{(s)}(0) = 1.84$ used in loop calculation. We emphasize the latter value results from assuming only the ω and ϕ contribute to $F_{KK^*}^{(s)}(t)$, whereas the former is obtained when *only* the ϕ' is included. Depending on the relative phase of the $(\rho\omega\phi)$ and $(\rho\omega\phi)'$ contributions in $e^+e^- \rightarrow KK\pi$, the ϕ' will either increase or decrease the point-like value (1.84) for this form factor by about 25%. At the KK^* threshold, the ϕ' contribution to $F_{KK^*}^{(s)}$ is about half as large as that from the ϕ , but becomes nearly five times larger in the vicinity of $t = m_{\phi'}^2$. For purposes of estimating the t -dependence of $F_{KK^*}^{(s)}$ in the region $t > t_0$, then, inclusion of only the ϕ' appears to be a reasonable approximation⁶. We note in passing that our estimate of the ϕ' contribution carries an uncertainty of 25% or more, as the experimental values for $\Gamma(\phi' \rightarrow KK\pi, e^+e^-)$ carry experimental errors of $\geq 25\%$ [28].

The implications of e^+e^- data for $F_{K^*}^{(s)}(t)$ are less clear. To our knowledge, there exists no annihilation data giving K^*K^* branching ratios. In $e^+e^- \rightarrow KK\pi\pi$ ($1.4 \leq \sqrt{s} \leq 2.18$), for example, the $K\pi$ invariant mass distribution is consistent with production of only one K^* per event [29]. Consequently, the data cannot be used to infer a K^* EM or strangeness form factor for $t > t_0$, and we must rely on a model. Given the evidence for ϕ' dominance of $F_{KK^*}^{(s)}(t)$ and for ϕ dominance of $F_K^{(s)}(t)$ as well as the absence of experimental observation of any $0^-(1^{--})$ $s\bar{s}$ mesons with mass $\geq 2m_{K^*}$, it is natural to assume that the t -dependence of $F_{K^*}^{(s)}(t)$ is governed by the tails of the known $s\bar{s}$ vector mesons. For simplicity, we include only one $s\bar{s}$ resonance – either the ϕ or the ϕ' – using the form of Eq. (20). The normalization $F_{K^*}^0 = |Q_{K^*}|$. In the DR results displayed in Table I, we quote a range of values, the limits of which correspond to using either the ϕ or ϕ' . A more realistic parameterization of $F_{K^*}^{(s)}(t)$ is likely to include some linear combination of ϕ and ϕ' poles, as well as small contributions from the ω and ω' . Existing information does not permit us to determine this linear combination. Consequently, we use the ranges appearing in Table I to estimate the uncertainty in the K^*K^* contribution associated with lack of knowledge of the K^* strangeness form factor.

⁶A more sophisticated treatment, including the tails of the ϕ and ω , would – as in the purely EM case – affect the shape of the form factor near the ϕ' peak and the resultant KK^* spectral function.

For the intermediate hyperon form factors, we are aware of no electromagnetic data to provide guidance for the choice of $F_n^{(s)}(t)$. We therefore work in analogy with the proton EM form factors, since both $F_B^{(s)}(t)$ ($B = \Lambda, \Sigma$) and $F_{PROTON}^{EM}(t)$ involve matrix elements of vector currents having unit conserved charge in the states of interest. Consequently, we adopt the standard dipole form factor for the Dirac strangeness form factors of the intermediate hyperons. Since the corresponding strange magnetic couplings are unknown, we omit magnetic form factors altogether. Because the resulting contributions to the strangeness moments are generally small compared to the mesonic contributions, we do not expect the uncertainty associated with $F_B^{(s)}(t)$ to be problematic.

Under these assumptions, our calculation proceeds as follows. The spectral functions entering Eqs. (17) have the general form

$$\text{Im } F(t) = \text{Re} \left[A_{J=1}^n(t) F_n^{(s)}(t)^* \right] = |A_{J=1}^n(t)| |F_n^{(s)}(t)| (1 + \gamma_n), \quad (24)$$

where $A_{J=1}^n$ is the appropriate combination of $J = 1$ partial waves for the process $n \rightarrow N\bar{N}$ and γ_n is a correction arising from the difference in phases between the amplitude $A_{J=1}^n$ and $F_n^{(s)}$ [16]. This correction can vary between -2 and 0 and depends on t . At present, we are unable to determine γ_n for the intermediate states considered here, and set $\gamma_n = 0$ to obtain an upper bound.

To compute the $A_{J=1}^n(t)$ in Born approximation, we calculate the imaginary parts of the diagrams (a) and (b) in Fig. 1 assuming point-like strangeness form factors, $F_n^{(s)}(t) \equiv 1$. We neglect the hyperon-nucleon mass difference and take $m_Y = m_N$. The seagull diagrams do not have an imaginary part, so we obtain no contributions from diagrams 1c. Furthermore, from Eq. (18) the individual contributions are manifestly gauge invariant in this approach. We calculate the imaginary parts of the corresponding diagrams with cutting rules [31] and insert them into the dispersion relations Eqs. (17). To obtain the imaginary parts it is convenient to consider the crossed t -channel matrix element $\langle N(p); \bar{N}(\bar{p}) | \bar{s} \gamma_\mu s | 0 \rangle$. The generic form of such a diagram is shown in Fig. 2. The different choices for the internal lines I, II, and III are shown in Table II. The equivalent of the previous kaon loop result is recovered if the internal lines are chosen as in case 1 and 2. In the following, we outline our calculation for the cases 3 - 5. In case 3 and 4, both kaons have been replaced by K^* vector mesons, while one kaon and one K^* contribute in case 5.

We choose to work in the center-of-momentum (CM) frame of the nucleon-antinucleon pair, where $q = (\omega, \vec{0})$. The loop diagrams lead to a physical reaction for $t \geq 4m_N^2$, which is the minimal energy required for the creation of a $\bar{N}N$ -pair, and we have $p' = (\omega/2, \vec{p}')$ and $p = (\omega/2, -\vec{p}')$ with $p_t = |\vec{p}'| = \sqrt{t/4 - m_N^2}$. We define the contribution of a particular Feynman diagram with vertex function Γ_μ as

$$\mathcal{M}_\mu^{(i)} = -i \bar{u}(p') \Gamma_\mu^{(i)} v(p). \quad (25)$$

These vertex functions are then multiplied by the strangeness form factor $|F^{(s)}(t)_{VDM}|$ from above as indicated by Eq. (24). Our choice for the momenta of the internal lines is indicated in Fig. 2.

For the cases 3 - 5 we obtain the vertex functions shown in Appendix B. The imaginary part of $\Gamma_\mu^{(i)}$ is always finite; hence, the divergencies of the d^4k integrals are without consequences. The vertex functions Γ^μ have branch cuts on the real axis for $t \geq (m_I + m_{II})^2$.

Their real part is continuous, such that the discontinuity associated with the cut is reflected only in the imaginary part. In the CM-frame of the nucleon and antinucleon, we have to calculate

$$\text{Im } \Gamma^\mu = \frac{1}{2i} \Delta \Gamma^\mu = \frac{1}{2i} \lim_{\delta \rightarrow 0} (\Gamma^\mu(\omega + i\delta) - \Gamma^\mu(\omega - i\delta)) . \quad (26)$$

In particular, we obtain the discontinuity $\Delta \Gamma^\mu$ using the Cutkosky rules [31] by cutting the lines I and II, i.e. by replacing the propagators of these lines by δ functions,

$$\frac{1}{p^2 - m^2 + i\varepsilon} \longrightarrow -2\pi i \theta(p_0) \delta(p^2 - m^2) . \quad (27)$$

As a consequence, the discontinuity arises when the particles I and II in Fig. 2 are on-shell. Due to the delta functions, the d^4k integration covers only a finite part of the k space, leading to a finite value of the integral. Next we write d^4k as $dk_0 k^2 dk d\Omega_k$ and use the delta functions to carry out the dk_0 and dk integrations. Moreover, the $d\Omega_k$ integration involves only x , the cosine of the angle between \vec{k} and \vec{p}' . The denominator of the remaining propagator acquires the structure $z + x$, where z depends on the particles internal to the loop.

$$\text{Case 3} \quad : \quad z = \frac{2(2m_N^2 - m_{K^*}^2) - t}{4p_t^2} = -(1 + \frac{m_{K^*}^2}{2p_t^2}) \quad (28)$$

$$\text{Case 4} \quad : \quad z = \frac{2m_{K^*}^2 - t}{4p_t q_t} \quad (29)$$

$$q_t = \sqrt{t/4 - m_{K^*}^2}$$

$$\text{Case 5} \quad : \quad z = \frac{m_K^2 + m_{K^*}^2 - 2q_t^2 - 2\sqrt{(q_t^2 + m_K^2)(q_t^2 + m_{K^*}^2)} - t}{8p_t q_t} \quad (30)$$

$$q_t = \frac{1}{2\sqrt{t}} \sqrt{t^2 + (m_{K^*}^2 - m_K^2)^2 - 2t(m_{K^*}^2 + m_K^2)}$$

Finally, $\text{Im } \Gamma_\mu$ can be expressed through Legendre functions of the second kind, and, using the relation

$$\text{Im } \Gamma_\mu = \gamma_\mu \text{Im } F_1 + i \frac{\sigma_{\mu\nu}}{2m} q^\nu \text{Im } F_2 , \quad (31)$$

the contributions to the imaginary parts of the Dirac and Pauli form factors for $t \geq 4m_N^2$, respectively, can be identified. The emerging spectral functions are valid for $t \geq 4m_N^2$. The dispersion integrals, however, start at $t_0 = (m_I + m_{II})^2$, with m_I and m_{II} the masses of the loop particles I and II, respectively. Consequently, the imaginary parts of the diagrams with two internal meson lines have to be analytically continued into the unphysical region $(m_I + m_{II})^2 \leq t < 4m_N^2$, by replacing the momentum $p_t = \sqrt{t/4 - m_N^2}$ by $i p_- = i\sqrt{m_N^2 - t/4}$. Similarly, the variables z become complex ($z \rightarrow i\xi$), and the Legendre functions of the second kind must be analytically continued as well.

Inserting now the imaginary parts and their analytical continuations in the unphysical region into the dispersion relations of Eq. (17), we obtain the KK^* and K^*K^* contributions

to the strangeness form factors of the nucleon. In particular, the dispersion relations for the K^* loop contributions to the strangeness radius and magnetic moment read

$$\langle r_s^2 \rangle_D = \frac{6}{\pi} \int_{t_0}^{\infty} dt \frac{\text{Im} F_1^{(s)}(t)}{t^2} \quad (32)$$

$$\mu^{(s)} = \frac{1}{\pi} \int_{t_0}^{\infty} dt \frac{\text{Im} F_2^{(s)}(t)}{t}, \quad (33)$$

where $\langle r_s^2 \rangle_D$ is related to the Sachs radius via Eq. (6). For most of the intermediate states considered here, the dispersion integrals in Eqs. (32, 33) converge when a non-pointlike form for the $F_n^{(s)}(t)$ is employed. However, the tensor K^*NB ($B = \Lambda, \Sigma$) coupling renders the K^*K^* divergent even when the VDM form factor is included. To regulate this integral, we note that the unitarity of the S-matrix implies that the $N\bar{N} \rightarrow K^*K^*$ amplitude is bounded in magnitude for scattering in the physical region, $t > 4m_N^2$. The Born approximation for this amplitude does not respect this boundedness property, signalling the importance of higher-order rescattering corrections [16]. At present, since we wish only to obtain an estimate for the K^* contributions, we replace the $A_{J=1}^n(t > 4m_N^2)$ by its value at the physical threshold, $A_{J=1}^n(t = 4m_N^2)$. We make the same replacement in the integrals for the KK^* intermediate state. This procedure leads to a crude upper bound on the contribution to the integrals from the integration region $t > 4m_N^2$.

The results of the DR estimates of the various contributions are quoted in Table I. The DR results for the $K\bar{K}$ contribution given in Table I were obtained using the rigorous unitarity bound. We stress that the K^* results give rough upper bounds on the various contributions, not only because of the boundedness of the strong amplitudes but also because the phase difference correction, γ_n , is not known. We also do not compute the total contributions from the various states, as we cannot presently determine their relative phases. Only in the one-loop calculation of the previous section are the relative phases fixed by the model.

IV. DISCUSSION AND CONCLUSIONS

The results shown in Table I illustrate the two primary conclusions of our analysis: (i) contributions from higher mass intermediate states to the strangeness moments are not necessarily small compared with those from the lightest ‘‘OZI allowed’’ state $K\bar{K}$; (ii) estimating these higher mass contributions can entail a significant degree of theoretical uncertainty.

In the one-loop model, the K^* contributions can be as much as an order of magnitude larger than those from the kaon loop. The origin of this result can be traced to two factors: the tensor coupling of the $N\Lambda K^*$ vertex is much larger than the $N\Lambda K$ coupling, and the cut-off of the Bonn form factor involving the K^* is about twice as large as that involving the kaon ($\Lambda_K = 1.2$ GeV). In the case of the former, omitting the tensor coupling reduces the contribution to the strangeness radius by a factor of five to ten and yields a near exact cancellation between the KK , KK^* , and K^*K^* contributions. In the case of the strange magnetic moment, the large K^*K^* and KK^* contributions drop by two orders of magnitude when κ is set to zero.

The effect of the larger cut-off is particularly emphasized in graphs which contain derivative (*i.e.* tensor) couplings of the K^* . These couplings bring in additional powers of the loop momentum k and the corresponding loop integrals therefore receive larger contributions from k of the order of the cut-off. However, the importance of loop momenta above ~ 2 GeV points to weaknesses of the one loop approximation. As we discuss in more detail below, the large $K^*K\Lambda$ and $K^*K^*\Lambda$ contributions (1b) appear to result from un-physical, un-realistically large values of the integrand for large loop momenta. Physically realistic contributions from these intermediate states are likely to be much smaller.

In fact, the DR contributions from the KK^* and K^*K^* states are significantly smaller in magnitude than those generated in the loop model, though they are still comparable to, or larger than, the $K\bar{K}$ contribution. The reduction in the magnitude of these contributions from the loop model estimate reflects two factors: the boundedness of the $n \rightarrow N\bar{N}$ scattering amplitude in the physical region and the presence of more realistic, non-pointlike $F_n^{(s)}(t)$. Although we have only implemented the boundedness crudely for the KK^* and K^*K^* states, the requirement that the partial waves are bounded in the physical region ($t > 4m_N^2$) is a rigorous one, following from the unitarity of the S-matrix. Since a one-loop calculation is equivalent to a DR in which the $F_n^{(s)}(t)$ are taken to be pointlike and the $A_{j=1}^n$ computed in the Born approximation, the one-loop results do not respect the boundedness requirement. The presence of hadronic form factors [Eqs. (9)] does not remedy this violation since they preserve the on-shell form for the $n \rightarrow N\bar{N}$ amplitudes.

In the $K\bar{K}$ case, the unitarity violation of the one-loop calculation was shown to be a serious one [16]. For the intermediate states containing a K^* , this violation appears to be all the more serious, as a comparison of the DR and loop results suggests. The tensor coupling of the K^* to baryons weights the $K^*K \rightarrow N\bar{N}$ and $K^*K^* \rightarrow N\bar{N}$ amplitudes more strongly in the physical region, relative to the un-physical region ($t_0 \leq t \leq 4m_N^2$), than in the $K\bar{K} \rightarrow N\bar{N}$ case. Consequently, the physical region contributes a substantial fraction of the entries (1b) for the K^*K and K^*K^* states (80% of the total in the K^*K^* case) – even after the imposition of a crude bound on the $A_{j=1}^n$ and inclusion of non-pointlike $F_K^{(s)}(t)$. Had we not imposed even our rough bound, the K^*K^* contribution to $\langle r_s^2 \rangle_D$, for example, would have been five times larger. We conclude that the large contributions to the strangeness moments resulting from the one-loop model are not physically realistic.

We emphasize that the DR calculation given here – though containing more physical information than the one-loop model – remains incomplete. A rigorous unitarity bound for the K^*K and K^*K^* amplitudes remains to be implemented, as has been done in the $K\bar{K}$ case. More importantly, the impact of higher order (in g) rescattering corrections and possible resonance effects in the $A_{j=1}^n(t_0 \leq t \leq 4m_N^2)$ must also be estimated. In the $K\bar{K}$ case, these effects significantly enhance the $\langle r_s^2 \rangle$ contribution over the entry $KK\Lambda$ (1b) in Table I [17]. This enhancement arises primarily from a near threshold $\phi(1020)$ -resonance in the $K\bar{K} \rightarrow N\bar{N}$ amplitude. Similarly, we expect inclusion of K^*K and K^*K^* rescattering and ϕ' resonance effects in the $A_{j=1}^n$ to modify the K^*K and K^*K^* entries in Table I. Unfortunately, sufficient $KK\pi \rightarrow N\bar{N}$ (or $KN \rightarrow K\pi N$) and $KK\pi\pi \rightarrow N\bar{N}$ ($KN \rightarrow KN\pi\pi$ *etc.*) data do not presently exist to afford a model-independent determination of these effects.

Given that higher mass contributions to the strangeness moments need not be small

compared to that from the $K\bar{K}$, it is desirable to reduce the theoretical uncertainty in the former as much as possible. The $K^*K^*\Lambda$ (1b) entry hints at the level of this uncertainty. Our “reasonable range” for this contribution allows for about a factor of four to seven variation, which follows from the choice of different, but reasonable, K^* strangeness form factors. Based on our previous study of the $K\bar{K}$ contribution, as well as the behavior of the scattering amplitudes in the physical region, we may reasonably expect a similar level of uncertainty associated with the presently unknown rescattering and resonance effects in the $A_{J=1}^{K^*K, K^*K^*}$.

To summarize, we have estimated K^*K and K^*K^* contributions to the nucleon strangeness moments, using two approaches which complement the quark model calculation of Ref. [14]. Our results confirm the conclusions reached in that work that higher mass hadronic states can be as important as the $K\bar{K}$ state and that a calculation of the strangeness moments based on a truncation in ΔE is not reliable. Similarly, we illustrate the significant theoretical ambiguities involved in estimating these higher mass contributions – particularly those associated with effects going beyond $\mathcal{O}(g^2)$ and with the intermediate state strangeness form factors. In this study, we have taken the first steps toward including the latter in a realistic way. We find that inclusion of physically reasonable parameterizations of the $F_n^{(s)}(t)$ can appreciably affect the K^*K and K^*K^* contributions. Even here, however, our efforts are limited by a lack of existing EM data. In the case of higher-order and resonance effects in the strong amplitudes, it should be evident that simple models which do not account for them can produce physically unrealistic estimates of the higher mass intermediate state contributions. Clearly, more sophisticated approaches are needed in order to understand how $s\bar{s}$ pairs live as virtual hadronic states.

ACKNOWLEDGMENTS

We would like to thank D. Drechsel and N. Isgur for useful discussions. This work has been supported in part by FAPESP and CNPq. M.N. would like to thank the Institute for Nuclear Theory at the University of Washington for its hospitality and H.F. acknowledges an HCM grant from the European Union and a DFG habilitation fellowship. MJR-M has been supported in part under U.S. Department of Energy contracts # DE-FG06-90ER40561 and # DE-AC05-84ER40150 and under a National Science Foundation Young Investigator Award. HWH has been supported by the Deutsche Forschungsgemeinschaft (SFB 201) and the German Academic Exchange Service (Doktorandenstipendium HSP III/ AUFE).

APPENDIX A: VERTEX FUNCTIONS: LOOPS

In the following appendices we list the explicit expressions for the one-loop diagrams considered in Section II.

They are numbered as in the figures: (1a) for $M = K^*$ and $B = B' = \Lambda, \Sigma$; (1b) for $M = M' = K^*$ and $B = B' = \Lambda, \Sigma$; (1b) for $M = K$, $M' = K^*$, and $B = B' = \Lambda, \Sigma$; (1c) for $M = K^*$ and $B = B' = \Lambda, \Sigma$.

$$\Gamma_\mu^{(1a)}(p', p) = ig_v^2 Q_B \int \frac{d^4 k}{(2\pi)^4} (F(k^2))^2 D^{\alpha\beta}(k) \left(\gamma_\alpha + i \frac{\kappa}{2m_N} \sigma_{\alpha\nu} k^\nu \right) S(p' - k) \gamma_\mu \times \\ S(p - k) \left(\gamma_\beta - i \frac{\kappa}{2m_N} \sigma_{\beta\gamma} k^\gamma \right), \quad (\text{A1})$$

$$\Gamma_\mu^{(1b)}(p', p) = -ig_v^2 Q_{K^*} \int \frac{d^4 k}{(2\pi)^4} F((k+q)^2) F(k^2) D^{\alpha\lambda}(k+q) D^{\sigma\beta}(k) (\gamma_\alpha + \\ + i \frac{\kappa}{2m_N} \sigma_{\alpha\nu} (k+q)^\nu) [(2k+q)_\mu g_{\sigma\lambda} - (k+q)_\sigma g_{\lambda\mu} - k_\lambda g_{\sigma\mu}] \times \\ S(p - k) \left(\gamma_\beta - i \frac{\kappa}{2m_N} \sigma_{\beta\gamma} k^\gamma \right), \text{ for } M = M' = K^* \\ = -\frac{g_v g_{ps} F_{K^* K}^{(s)}(0)}{m_{K^*}} \epsilon_{\mu\nu\lambda\alpha} \int \frac{d^4 k}{(2\pi)^4} \left\{ F((k+q)^2) F_K(k^2) D^{\alpha\beta}(k+q) \times \right. \\ \Delta(k^2) (k+q)^\nu k^\lambda \left(\gamma_\beta + i \frac{\kappa}{2m_N} \sigma_{\beta\delta} (k+q)^\delta \right) S(p - k) \gamma_5 + \\ \left. + F(k^2) F_K((k+q)^2) D^{\alpha\beta}(k) \Delta((k+q)^2) k^\nu (k+q)^\lambda \gamma_5 \times \right. \\ \left. S(p - k) \left(\gamma_\beta - i \frac{\kappa}{2m_N} \sigma_{\beta\delta} k^\delta \right) \right\}, \text{ for } M = K, M' = K^* \quad (\text{A2})$$

$$\Gamma_\mu^{(1c)}(p', p) = g_v^2 Q_{K^*} \int \frac{d^4 k}{(2\pi)^4} F(k^2) D^{\alpha\beta}(k) \left\{ i \left[\frac{(q+2k)_\mu}{(q+k)^2 - k^2} (F(k^2) - F((k+q)^2)) \times \right. \right. \\ \left. \left(\gamma_\alpha + i \frac{\kappa}{2m_N} \sigma_{\alpha\nu} k^\nu \right) S(p - k) \left(\gamma_\beta - i \frac{\kappa}{2m_N} \sigma_{\beta\gamma} k^\gamma \right) - \frac{(q-2k)_\mu}{(q-k)^2 - k^2} (F(k^2) + \right. \\ \left. - F((k-q)^2)) \left(\gamma_\alpha + i \frac{\kappa}{2m_N} \sigma_{\alpha\nu} k^\nu \right) S(p' - k) \left(\gamma_\beta - i \frac{\kappa}{2m_N} \sigma_{\beta\gamma} k^\gamma \right) \right] + \\ \left. + \frac{\kappa}{2m_N} \left[F((k+q)^2) \sigma_{\alpha\mu} S(p - k) \left(\gamma_\beta - i \frac{\kappa}{2m_N} \sigma_{\beta\gamma} k^\gamma \right) + \right. \right. \\ \left. \left. - F((k-q)^2) \left(\gamma_\alpha + i \frac{\kappa}{2m_N} \sigma_{\alpha\nu} k^\nu \right) S(p' - k) \sigma_{\beta\mu} \right] \right\}, \quad (\text{A3})$$

In the above equations we define $p' = p + q$ and use the notation $D_{\alpha\beta}(k) = (-g_{\alpha\beta} + k_\alpha k_\beta / m_{K^*}^2) (k^2 - m_{K^*}^2 + i\epsilon)^{-1}$ for the K^* propagator, $\Delta(k^2) = (k^2 - m_K^2 + i\epsilon)^{-1}$ for the kaon propagator, $S(p - k) = (\not{p} - \not{k} - m_B + i\epsilon)^{-1}$ for the hyperon, B , propagator with mass $m_\Lambda = 1116$ MeV, $m_\Sigma = 1193$ MeV and strangeness charge $Q_B = 1$.

APPENDIX B: VERTEX FUNCTIONS: DISPERSION CALCULATION

Here, we display the vertex functions for the dispersion relation calculation of Section III. We require the product of propagator denominators and $|F^{(s)}(t)_{VDM}|$ for the cases 3-5. This product is abbreviated by

$$\mathcal{D}_3 = \left\{ [(k - q/2)^2 - m_N^2 - i\epsilon][(k + q/2)^2 - m_N^2 - i\epsilon] \right. \\ \left. [(p' - k - q/2)^2 - m_{K^*}^2 - i\epsilon] \right\}^{-1} |F^{(s)}(t)_{VDM}|, \quad (\text{B1})$$

for case 3 and accordingly for cases 4 and 5. The vertex functions are labelled as in section III (Table I). We obtain:

Case 3 (K^*K^*B 1a) :

$$\Gamma_\mu^{(3)} = -iQ_B g_v^2 \int \frac{d^4k}{(2\pi)^4} \left(\gamma_\alpha + \frac{i\kappa}{2m_N} \sigma_{\alpha\nu} (p' - k - q/2)^\nu \right) \\ (\not{k} + \not{q}/2 + m_N) \gamma_\mu (\not{k} - \not{q}/2 + m_N) \\ \left(\gamma_{\alpha'} - \frac{i\kappa}{2m_N} \sigma_{\alpha'\nu'} (p' - k - q/2)^{\nu'} \right) \\ (g^{\alpha\alpha'} - (p' - k - q/2)^\alpha (p' - k - q/2)^{\alpha'} / m_{K^*}^2) \mathcal{D}_3 \quad (\text{B2})$$

Case 4 (K^*K^*B 1b) :

$$\Gamma_\mu^{(4)} = -iQ_{K^*} g_v^2 \int \frac{d^4k}{(2\pi)^4} \left(\gamma_{\beta'} + \frac{i\kappa}{2m_N} \sigma_{\beta'\nu} (k + q/2)^\nu \right) \\ (g^{\beta'\beta} - (k + q/2)^{\beta'} (k + q/2)^\beta / m_{K^*}^2) \\ (g^{\alpha\alpha'} - (k - q/2)^\alpha (k - q/2)^{\alpha'} / m_{K^*}^2) (\not{p}' - \not{k} - \not{q}/2 + m_N) \\ (2k_\mu g_{\beta\alpha} - g_{\beta\mu} (k + q/2)_\alpha - g_{\alpha\mu} (k - q/2)_\beta) \\ \left(\gamma_{\alpha'} - \frac{i\kappa}{2m_N} \sigma_{\alpha'\nu'} (k - q/2)^{\nu'} \right) \mathcal{D}_4 \quad (\text{B3})$$

Case 5 (KK^*B 1b) :

$$\Gamma_\mu^{(5)} = -2g_{ps} g_v \frac{F_{K^*K}^{(s)}(0)}{m_{K^*}} \int \frac{d^4k}{(2\pi)^4} \left(\gamma_{\beta'} + \frac{i\kappa}{2m_N} \sigma_{\beta'\nu} (k + q/2)^\nu \right) \\ (g^{\beta'\beta} - (k + q/2)^{\beta'} (k + q/2)^\beta / m_{K^*}^2) \\ \epsilon_{\sigma\beta\rho\mu} (k + q/2)^\sigma q^\rho (\not{p}' - \not{k} - \not{q}/2 + m_N) \gamma_5 \mathcal{D}_5 \quad (\text{B4})$$

REFERENCES

- [1] P. Geiger and N. Isgur, *Phys. Rev.* **D41** (1990) 1595.
- [2] P. Geiger and N. Isgur, *Phys. Rev.* **D44** (1991) 799; *Phys. Rev. Lett.* **67** (1991) 1066; *Phys. Rev.* **D47** (1993) 5050; P. Geiger, *Phys. Rev.* **D49** (1994) 6003.
- [3] D. B. Kaplan and A. Manohar, *Nucl. Phys.* **B310** (1988) 527.
- [4] T. P. Cheng, *Phys. Rev.* **D13** (1976) 2161; J. Gasser, H. Leutwyler, and M. E. Sainio, *Phys. Lett.* **B168** (1986) 1051, *Phys. Lett.* **B253** (1991) 252.
- [5] EMC Collaboration, J. Ashman *et al.*, *Nucl. Phys.* **B328** (1989)1; E142 Collaboration, P. L. Anthony *et al.*, *Phys. Rev. Lett.* **71** (1993) 959; SMC Collaboration, B. Adeva *et al.*, *Phys. Lett.* **B302** (1993) 53; SMC Collaboration, D. Adams *et al.*, *Phys. Lett.* **B329** (1994) 399; E143 Collaboration, K. Abe *et al.*, *Phys. Rev. Lett.* **74** (1995) 346.
- [6] L. A. Ahrens *et al.*, *Phys. Rev.* **D35** (1987) 785.
- [7] B. Mueller *et al.*, *Phys Rev. Lett.* **78** (1997) 3824; MIT-Bates Report No. 94-11, M. Pitt and E.J. Beise, spokespersons.
- [8] Mainz-MAMI Report No. A4/1-93, D. von Harrach, spokesperson.
- [9] TJNAF Report No. PR-91-017, D.H. Beck, spokesperson; TJNAF Report No. PR-91-004, E.J. Beise, spokesperson; TJNAF Report No. PR-91-010, J.M. Finn and P.A. Souder, spokespersons.
- [10] D. B. Leinweber, *Phys. Rev.* **D53** (1996) 5115; K.-F. Liu, U. of Kentucky preprint UK/95-11, 1995; S.J. Dong, K.F. Liu, and A.G. Williams, [hep-ph/9712483].
- [11] N. W. Park, J. Schechter, and H. Weigel, *Phys. Rev.* **D43** (1991) 869; S.-T. Hong and B.-Y. Park, *Nucl. Phys.* **A561** (1993) 525; S. C. Phatak and S. Sahu, *Phys. Lett.* **B321** (1994) 11; W. Melnitchouk and M. Malheiro, *Phys. Rev.* **C55** (1997) 431.
- [12] R. L. Jaffe, *Phys. Lett.* **B229** (1989) 275; H.-W. Hammer, Ulf-G. Meißner and D. Drechsel, *Phys. Lett.* **B367** (1996) 323; H. Forkel, *Prog. Part. Nucl. Phys.* **36** (1996) 229; *Phys. Rev.* **C56** (1997) 510; M. J. Musolf, Eleventh Student Workshop on Electromagnetic Interactions, Bosen, Germany, 1994 (unpublished).
- [13] W. Koepf and E.M. Henley, *Phys.Rev.* **C49** (1994) 2219; W. Koepf, S.J. Pollock and E.M. Henley, *Phys. Lett.* **B288** (1992) 11; M.J. Musolf and M. Burkardt, *Z. Phys.* **C61** (1994) 433; T.D. Cohen, H. Forkel and M. Nielsen, *Phys. Lett.* **B316** (1993) 1; H. Forkel, M. Nielsen, X. Jin and T.D. Cohen, *Phys. Rev.* **C50** (1994) 3108.
- [14] P. Geiger and N. Isgur, *Phys. Rev.* **D55** (1997) 299.
- [15] M. J. Ramsey-Musolf and H. Ito, *Phys. Rev.* **C55** (1997) 3066.
- [16] M.J. Musolf, H.-W. Hammer, and D. Drechsel, *Phys. Rev.* **D55** (1997) 2741.
- [17] M. J. Ramsey-Musolf and H.-W. Hammer, INT Report No. DOE/ER/40561-323-INT97-00-170 [hep-ph/9705409], to appear in *Phys. Rev. Lett.* .
- [18] H.-W. Hammer and M.J. Ramsey-Musolf, *Phys. Lett.* **B416** (1998) 5.
- [19] B. Holzenkamp, K. Holinde and J. Speth, *Nucl. Phys.* **A500** (1989) 485.
- [20] Particle Data Group, Review of Particle Physics, *Phys. Rev.* **D54** (1996) 1.
- [21] K. Ohta, *Phys. Rev.* **D35** (1987) 785.
- [22] S. Wang and M.K. Banerjee, *Phys. Rev.* **C54** (1996) 2883.
- [23] J.L. Goity, M.J. Musolf, *Phys. Rev.* **C53** (1996) 399.
- [24] P. Jain *et al.*, *Phys. Rev.* **D37** (1988) 3252.

- [25] B. Delcourt *et al.*, *Phys. Lett.* **B99** (1981) 257; F. Mane *et al.*, *Phys. Lett.* **B94** (1981) 261; F. Felicetti and Y. Srivastava, *Phys. Lett.* **B107** (1981) 227.
- [26] F. Mane *et al.*, *Phys. Lett.* **B112** (1982) 178.
- [27] J. Buon *et al.*, *Phys. Lett.* **B118** (1982) 221.
- [28] A. B. Clegg and A. Donnachie, *Z. für Phys.* **C62** (1994) 455.
- [29] A. Cordier *et al.*, *Phys. Lett.* **B110** (1982) 335.
- [30] D. Bisello *et al.*, *Z. für Phys.* **C52** (1991) 227.
- [31] R.E. Cutkostky, *J. Math. Phys.* **1** (1960) 429; see also C. Itzykson and J.B. Zuber, *Quantum Field Theory*, Mc-Graw-Hill, New York, 1980.

TABLES

Contribution	$\langle r_s^2 \rangle_D$ (fm ²) loop	$ \langle r_s^2 \rangle_D $ (fm ²) DR	μ_s loop	$ \mu_s $ DR
<i>KKB</i> 1a	0.006	0.001	-0.107	0.023
<i>KKB</i> 1b	-0.009	0.036	-0.078	0.143
<i>KKB</i> 1c	-0.004	0	-0.069	0
<i>KKB</i> tot	-0.007		-0.24	
<i>K*K*B</i> 1a	0.075	0.001	-2.283	0.053
<i>K*K*B</i> 1b	-0.038	0.003 \rightarrow 0.012	-2.343	0.059 \rightarrow 0.408
<i>K*K*B</i> 1c	-0.007	0	0.499	0
<i>K*K*B</i> tot	0.030		-4.127	
<i>KK*B</i> 1b	0.078	0.035	1.015	0.425
total	0.101		-3.352	

TABLE I. Intermediate state contributions to the strange magnetic moment μ_s and the electric strangeness radius $\langle r_s^2 \rangle_D$. The contributions are labelled according to the diagrams in Fig. 1 and the intermediate state particles.

Case	I	II	III
1	<i>K</i>	<i>K</i>	Λ, Σ
2	Λ, Σ	Λ, Σ	<i>K</i>
3	Λ, Σ	Λ, Σ	<i>K*</i>
4	<i>K*</i>	<i>K*</i>	Λ, Σ
5	<i>K</i>	<i>K*</i>	Λ, Σ

TABLE II. Particles assigned to the internal lines in the loop diagram of Fig. 2.

FIGURES

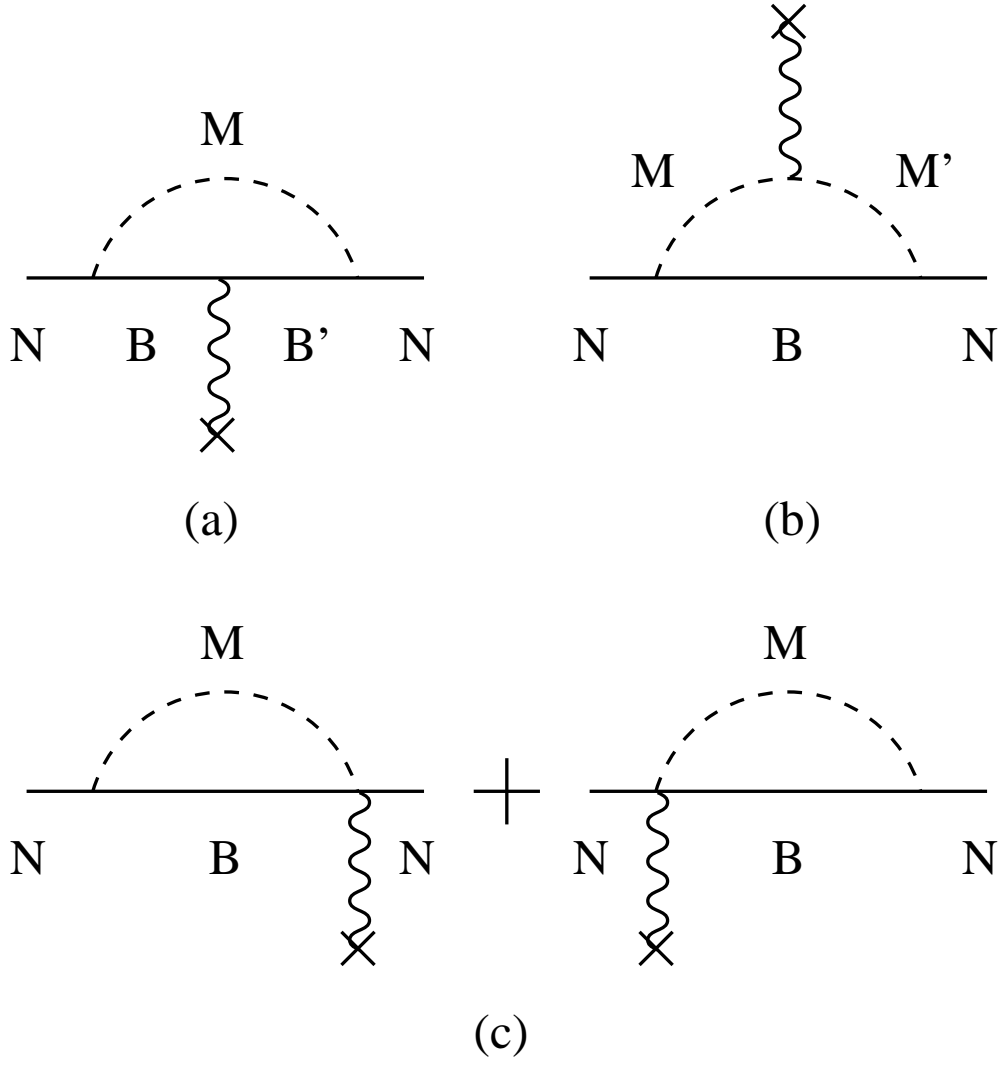


FIG. 1. Diagrams representing KB and K^*B contributions to nucleon strangeness form factors. Solid line represents baryon (B) and dashed line indicates meson (M, M'). Fig. (1a) gives $B\bar{B}$ contribution; (1b) gives $K\bar{K}$, K^*K , and K^*K^* contributions; (1c) indicates seagull contributions required by gauge invariance.

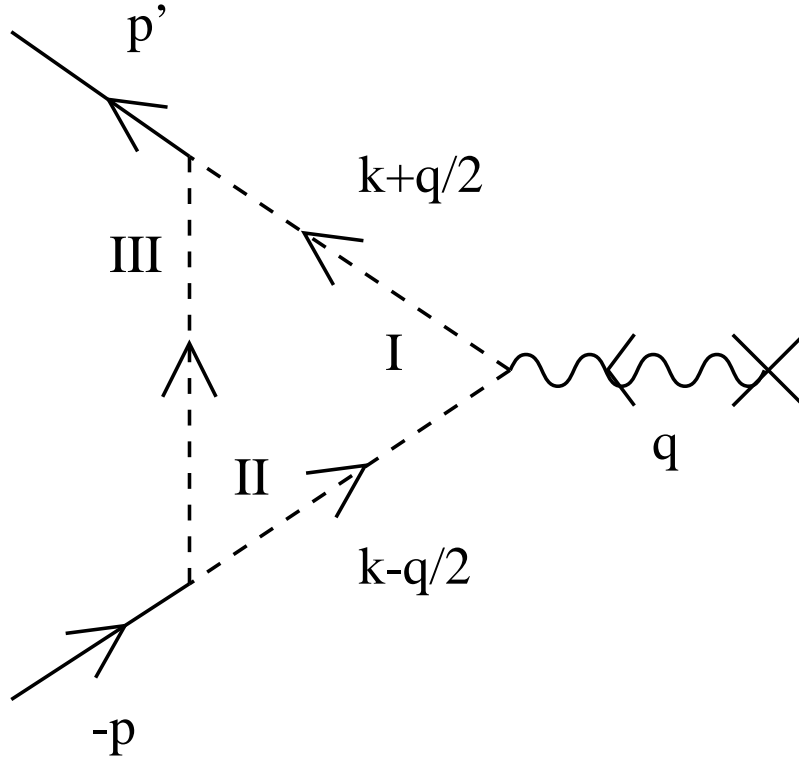


FIG. 2. General form of the calculated loop diagrams. The various combinations of intermediate particles considered in our calculation are listed in Table II.